

Provided for non-commercial research and education use.
Not for reproduction, distribution or commercial use.



This article was published in an Elsevier journal. The attached copy is furnished to the author for non-commercial research and education use, including for instruction at the author's institution, sharing with colleagues and providing to institution administration.

Other uses, including reproduction and distribution, or selling or licensing copies, or posting to personal, institutional or third party websites are prohibited.

In most cases authors are permitted to post their version of the article (e.g. in Word or Tex form) to their personal website or institutional repository. Authors requiring further information regarding Elsevier's archiving and manuscript policies are encouraged to visit:

<http://www.elsevier.com/copyright>



ELSEVIER

Available online at www.sciencedirect.com

Journal of African Earth Sciences 50 (2008) 37–48

 Journal of African
Earth Sciences

www.elsevier.com/locate/jafrearsci

Tidal flat sedimentation during the last millennium in the northern area of Tidra Island, Banc d'Arguin, Mauritania

Ulrike Proske ^{a,*}, Till J.J. Hanebuth ^{a,b}, Helge Meggers ^{a,b}, Suzanne A.G. Leroy ^c^a University of Bremen, Faculty of Geosciences, Department of Sedimentology, Klagenfurter Strasse, 28359 Bremen, Germany^b RCOM-Research Center Ocean Margins, Marum Building, Leobener Straße, 28359 Bremen, Germany^c Institute for the Environment, Brunel University, Uxbridge UB8 3PH, UK

Received 1 March 2007; received in revised form 20 August 2007; accepted 14 September 2007

Available online 22 September 2007

Abstract

The area around the Tidra Island is a complex and highly dynamic clastic tidal flat system. The character of the northern part of this area is outlined, together with its sedimentary changes through time and the different depositional environments that shaped this coastal area in the last centuries are reconstructed. The multi-proxy approach together with ¹⁴C-dating has led to the identification of four main types of deposits using the modern facies distribution as an analogue:

- (a) A ~800–440 cal yr BP old sandy shoreface,
- (b) different types of tidal flats (sand to mudflat) that discontinuously developed on top of this older shoreface deposit,
- (c) seagrass stands in the most recent part of the sedimentary succession and
- (d) at least two storm deposits of various ages within the record.

The interpretation of the cores' highly non-continuous succession allows the postulation of a constructive sandy shoreface that covered large parts of the area. The in most cases erosive boundary between this older deposit and the overlying tidal flat deposits indicates that a short-lived event eroded parts of this sandy shoreface deposit. According to the latest studies, recent sea-level fluctuations can be excluded so it is suggested that a major storm event eroded parts of the sandy shoreface to about 2–2.5 m below the modern mean low water. This erosive storm event possibly produced accommodation space in the water column for the renewed accumulation of sediments so that tidal flat sediments could evolve on top of the sandy shoreface deposits. At least one other storm event led to further reshaping of the area and finally the modern tidal flats and seagrass stands in the proximity of Tidra Island formed. As shown in current research [e.g. Barousseau, J.P., Vernet, R., Saliège, J.F., Descamps, C., 2007. Late Holocene sedimentary forcing and human settlements in the Jerf el Oustani – Ras el Sass region (Banc d'Arguin, Mauritania). *Geomorphologie-Relief Processus Environnement* 1, 7–18], these observations are in contrast to the overall constructive coastline evolution the Golfe d'Arguin. This is probably linked to the exceptional position of the Tidra Island area that represents a morphological protrusion in the coastline and is thus also exposed to erosive processes rather than sediment accumulation.

© 2007 Elsevier Ltd. All rights reserved.

Keywords: Banc d'Arguin; Tidra Island; Tidal flat; Latest Holocene; Storm events

1. Introduction

Located on the coast of Mauritania, the Banc d'Arguin forms a shallow-water and partly tidal flat area, constitut-

ing a major part of the larger Golfe d'Arguin (21°10'–19°20' N, 17°20'–16°15' W). The Golfe in turn is bounded by Cap Blanc in the North and Cap Timiris in the South (Fig. 1). The Banc area comprises many islands of different sizes (not all shown in Fig. 1) of which Tidra Island in the Southeast is the largest. This island is a desert being fringed by narrow sabkhas (Fig. 2). Its northern tip is famous for

* Corresponding author. Fax: +49 421 218 7431.

E-mail address: uproске@uni-bremen.de (U. Proske).

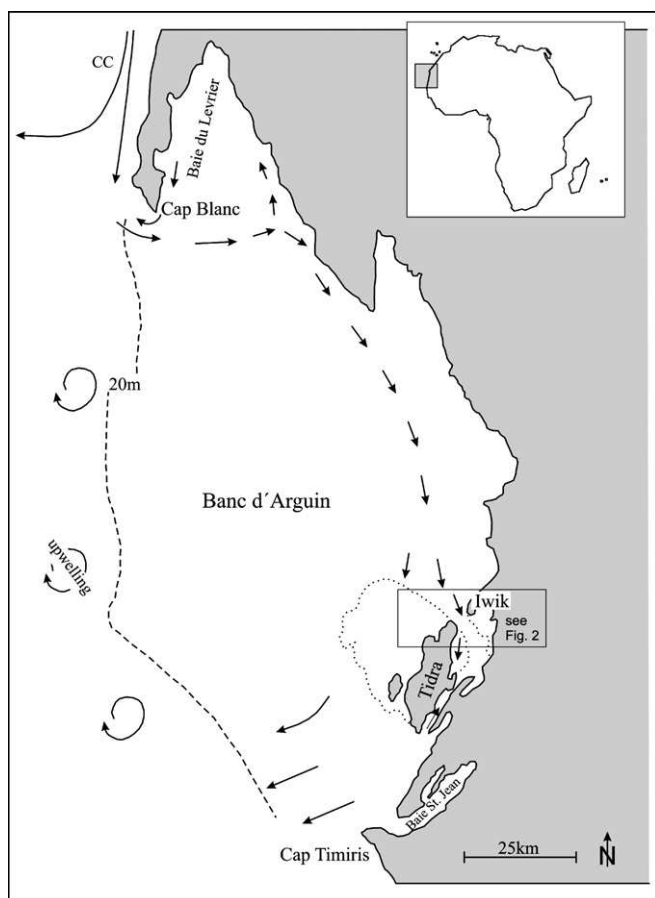


Fig. 1. Simplified map of the Banc d'Arguin and the geographic landmarks named in the text. The arrows indicate schematically the simplified flow of water masses described in the text. Also shown is the 20 m bathymetric line as well as the approximate coverage of the tidal flat area around Tidra (dotted line) (After: Sevrin-Reyssac, 1993 and Peters, 1976).

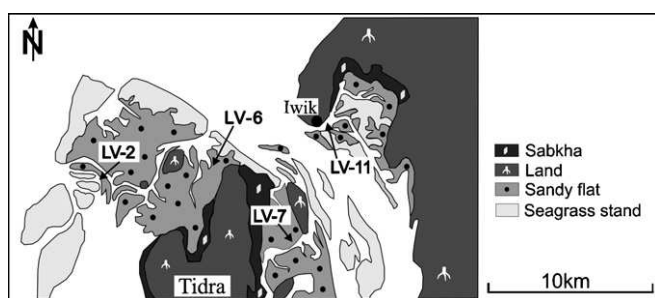


Fig. 2. Position of the core sampling sites within the tidal flat area and the facies types. The northern tip of Tidra and the village of Iwik are shown for orientation. (After: Michaelis and Wolff, 2001).

housing the northernmost mangroves in W-Africa (Dahdouh-Guebas and Koedam, 2001; Wolff and Smit, 1990). The supra-regional importance of the Banc d'Arguin as ecosystem led to the foundation of the National Park "Banc d'Arguin" in 1976 (Wolff et al., 1993b).

1.1. Hydrographical situation and climate

The Canary Current (CC) flows southward along the coast of NW- Africa and splits up in the proximity of Cap

Blanc (Fig. 1). The larger portion of this current flows in a south-westerly direction towards the open Atlantic, whilst a smaller branch mixes with upwelling waters. A part of this mixed water is transported into the Golfe d'Arguin, south of Cap Blanc. Within about 30 days these waters flow in a complicated pattern across the Banc d'Arguin (Dedah, 1993), leaving the area close to Cap Timiris (Fig. 1; Peters, 1976). On the outer shelf a sharp front between these warm and highly saline waters and the cold upwelling water is observed throughout the whole year, suggesting that no mixing of the water bodies occurs. The tide ranges mainly between 1 m (neap tide) and 2 m (spring tide) with exceptions up to 2.7 m (Wolff et al., 1993b). Together with wave action, the tidal stream causes a mixing of the water column with a maximum current speed of 1 m sec^{-1} in deeper channels (Wolff et al., 1993a). Precipitation is in general low with 50 mm/year or less in the Baie St. Jean (Stein, 1980). There are no recent rivers draining into the Banc, so the sediment supply is limited to wind transported material. The trade winds blow from northerly directions throughout the whole year but their strength varies seasonally. Extreme wind speeds of up to 65 m sec^{-1} have been recorded at Nouadhibou Airport (Dedah, 1993) for the time span 1953–1982 with an additional increase in dust storm days per year in the years after 1970 (Middleton, 1987). Seaward directed storms in bays are able to increase the orbital wave and the current velocities so that the upper layers of sediment in shallow areas ($<20 \text{ m}$ water depth) can get resuspended (e.g. Puig et al., 2007). When these strong winds coincide with high tides, associated storm surges can appear that lead to further intense sediment resuspension. In the case of the Golfe d'Arguin, especially the northerly storms can build up high wave fronts while travelling across the whole length of the Golfe. Due to the pronounced, exposed position of the Tidra Island and its surrounding shallow-water area these wave fronts can then strongly affect the region mainly on its northern rim.

1.2. The coastal area in the latest Holocene

Whether a series of subordinate sea-level fluctuations has affected the Mauritanian coast in the Holocene is still an object of discussion. According to Einsele et al. (1974) a major regression of 3 m along the Mauritanian coast could have occurred after the mid-Holocene sea-level highstand, followed by a minor transgression of 1.5 m around 3500 cal yr BP (cal yr BP = calendar years Before Present with "present" meaning 1950 A.D.; Fig. 3). Elouard et al. (in Barousseau et al. 1995) show comparable shifts in sea-level but their reconstruction is not exactly isochronal with the curve from Einsele et al. (1974). A more recent and thus more reliable study by Barousseau et al. (1995) suggests in contrast, that there is only one significant sea-level highstand around 5000 yr BP followed by one major regression to the modern level until 3000 yr BP (Fig. 3). Sea-level fluctuations that are younger than 3000 yr are not reported in this study.

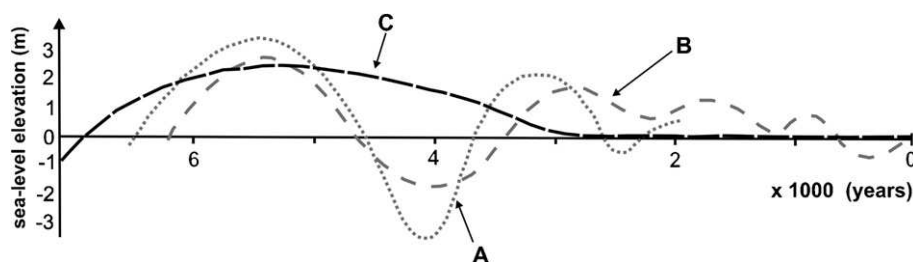


Fig. 3. The sea level fluctuations in the last 5000 years on the coast of Mauritania according to A – Einsele et al. (1974); B – Elouard et al. (1977); C – Barusseau et al. (1995). Simplified after Barusseau et al. (1995).

The area around Tidra Island was mainly affected by the “Nouakchottien”, a highstand in sea-level of 2–3 m (Elouard et al., 1969) parallel in time to the termination of the African Humid Period that ranged from ~11,500–5500 cal yr BP (e.g. DeMenocal et al., 2000; Gasse, 2005). This transgression left characteristic, thick coastal shell beds with an associated terminal aeolian sand layer both now positioned ~3.5 m above modern sea level (Einsele et al., 1974). In contrast to this, Barusseau et al. (2007) show that the Nouakchottien sea level did not rise above the modern level and thus could not have left any elevated deposits. Compared with the earlier work from the same author, this latest observation is contrary to the sea-level curve shown in Fig. 3 but since this study is focusing on much younger sediments, this possible sea level highstand ca. 5000 yr BP only plays a minor role for this work interpretation.

Concerning younger influences on the area, DeMenocal et al. (2000) show that the area off Cap Blanc experienced a decrease in sea surface temperature of ca. 3–4 °C and a reduced seasonality during the Little Ice Age (LIA, 1300–1870 A.D. or ~650–80 cal yr BP). Since Cap Blanc is the “entrance area” of the water flowing over the Banc d’Arguin the hydrographical conditions and thus sedimentation patterns on the Banc may also have been slightly modified to an unknown extent.

Since the 1960s various sedimentological studies were carried out on surface samples from the Baie du Lévrier (Koopmann et al., 1979) and Baie St. Jean (Stein, 1980) as well as in the whole Golfe d’Arguin area (Domain, 1977; Piessens, 1979) and along the coast of Mauritania (Einsele et al., 1974). The work of Einsele et al. (1974) in particular provides an overview of the lateral, depositional facies distribution in different environments and could thus be used to understand the appearance of palaeo-facies types in sedimentary sub-bottom successions (see chapter 3.2 for the introduction of Einsele et al.’s facies types). The latest investigation in the terrestrial part of the Banc d’Arguin shows continuous sediment accumulation in the area of Ras el Sass over the past ~5000 years (Barusseau et al., 2007).

The main purpose of this work is to investigate the character of the sediments in the proximity of Tidra Island by studying the various types of deposits. The changes in those sediments through time will provide information on the

spatial and temporal development of the investigated area. For a more general view it is important to understand the sedimentary dynamics in the whole tidal flat system of the Banc d’Arguin to judge its stability as an ecosystem.

2. Material and methods

During the “ICSU Dark Nature-IGCP490” coring campaign in 2004 Livingstone and Kajak corers were used to recover 18 sediment cores out of the proximate tidal flat area around Tidra Island and Iwik. The cores were taken during low tide just below the intertidal zone. Four out of those 18 cores (BA-04-LV-2, -6, -7 and -11, in the following text abbreviated as LV-2, LV-6 and so forth) were selected for further investigation (for core locations see Fig. 2). A first detailed visual description of the cores’ colour, grain size and internal structures was performed at Brunel University, London (UK). Thereafter, the cores were taken for X-ray imaging at the Diakoniekrankehaus Rotenburg/Wümme (Germany) to visualize internal sediment structures. Based on the visual core description, at least two samples were taken per sedimentological unit (approximately 25 samples per core) and measured for total organic carbon/total carbon (TOC/TC)- and carbonate (CaCO_3)-contents as well as sieved into the various sand subfractions. The fraction 500–125 μm of each sample was used for qualitative and quantitative microscopical analyses to gain information about the sediment content. Fractions >500 μm were briefly considered to gather further information about larger components. For core LV-2 nitrogen measurements with the Vario EL CHN Analyzer were carried out in order to calculate the C/N-ratio.

Carefully selected gastropod and bivalve shells (Table 1) were sampled to obtain five radiocarbon ages in three out of the four cores. The results were calibrated into calendar years with the program CALIB4.4.2 (Stuiver and Reimer, 1998). In this study a conservative reservoir age of 400 years for the correction of marine carbonate is assumed (Bard, 1988) because the influence of upwelling waters on the one hand and the amount of the intensive exchange of shallow waters with the atmosphere on the other hand cannot be determined. The raw as well as calibrated radiocarbon ages are shown in Table 2. Due to the young ages and the inflections of the calibration curve in this time period, the 2σ -range of the calibrated ages was used. The

Table 1
Overview of the dated shell material, the general habitat of the associated organism and references

Dated shell	Habitat	Example reference
<i>Turritella torulosa</i>	on or in the upper centimetres of soft to hardened mud grounds in ca. 10–200 m water depth	Fretter and Graham (1981)
<i>Calyptrea chinensis</i>	on soft substrate in the sublittoral zone in up to 20 m water depth	Fretter and Graham (1981)
<i>Abra tenuis</i>	on or in the upper centimetres of muddy substrate in the upper intertidal zone	Dekker and Beukema (1999)

Table 2
Conventional radiocarbon ages and 2σ -ranging, calibrated age data for the three cores

Core	Sample depth (cm)	Conventional age (yr BP)	Calibrated age (cal yr BP, 2σ)	Sampled material
LV-2	159	505 ± 25	50–240	Gastropod (<i>Turritella torulosa</i>)
	248	230 ± 30	690–870	Gastropod (<i>Turritella torulosa</i>)
LV-6	239	880 ± 35	440–550	Gastropod (<i>Calyptrea chinensis</i>)
LV-7	102	-775 ± 30	0	Gastropod (<i>Turritella torulosa</i>)
	204	530 ± 25	60–260	Bivalve (<i>Abra tenuis</i>)

negative conventional radiocarbon age for sample “LV-7, 102 cm” is interpreted as “modern” (meaning within the time span 1945–1963 A.D.). During these years the testing of nuclear bombs increased the atmospherical ^{14}C (e.g. Levin et al., 1985; Manning et al., 1990). Thus the conventional equation produces a negative age for shells being built in that time period. More information concerning age dating in comparable environments has not been available, so these calibrated ages are presented but with the caveat that they may be too old. Another problem can be that the ^{14}C -dating method might not be giving the most accurate results in this young time period. But since other dating methods that have been used in tidal flat environments, like ^{210}Pb and ^{137}Cs , only work for the last ~200 years (Roberts, 1989), we assume the radiocarbon method remains the most appropriate for the sequences.

3. Results

3.1. Sedimentary facies analyses

The four selected cores were processed with the same methods but due to the sake of clarity we only show here the detailed results exemplarily on core LV-7. The composite X-ray image as well as a remarkable part of the cores' Section 2 is shown to provide an overview of the deposits and their internal structures (Fig. 4). The different shades

of grey correspond to the mud content (increasing brightness indicates less mud) and can thus be used as an indicator of grain size. In general this core shows larger parts with clearly visible lamination (upper part of Section 2) and other parts that are intensely bioturbated (upper part of Section 1 and almost entire Section 3). Especially noteworthy are the lowermost ~10 cm of Section 1 where a rather bioturbated, muddy sediment unit changes sharply into a laminated sandy and muddy deposit illustrating an abrupt change in sedimentary pattern. The box within Fig. 4 shows a part of the cores' irregular lamination as well as some of the shell material.

Generally the values of the TOC and carbonate contents vary considerably throughout all cores. The TOC content reaches a maximum value of 2.3 wt.% whilst the minimum value is 0.1 wt.%. The carbonate content shows a maximum value of 18.0 wt.%, whereas the carbonate minimum value is 0.5 wt.%. Fig. 5a shows the variation of the TOC and carbonate content as well as the abundance of organic particles (i.e. plant fibres) and carbonate shells and the sand/mud ratio throughout core LV-7. The TOC-content runs, as expected, approximately parallel with the abundance of organic particles (counted in the merged fraction 500–125 μm). The highest TOC-values of ~2.3 wt.% are measured at the top of the core. Further downwards the subsequent decline in TOC-values down to ~0.3 wt.% can be observed. The carbonate content and the number

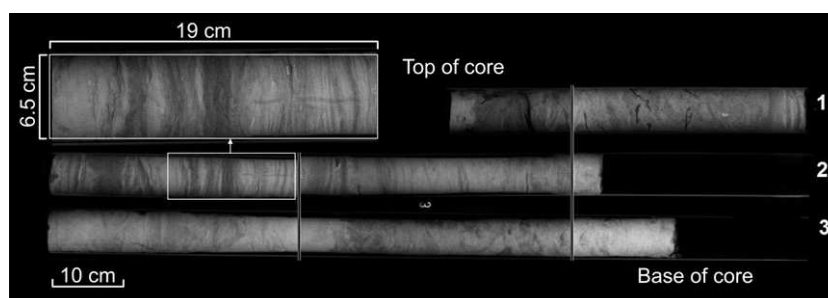


Fig. 4. Composite X-ray image and detail (white box) of core LV-7. The individual core sections are labelled with numbers.

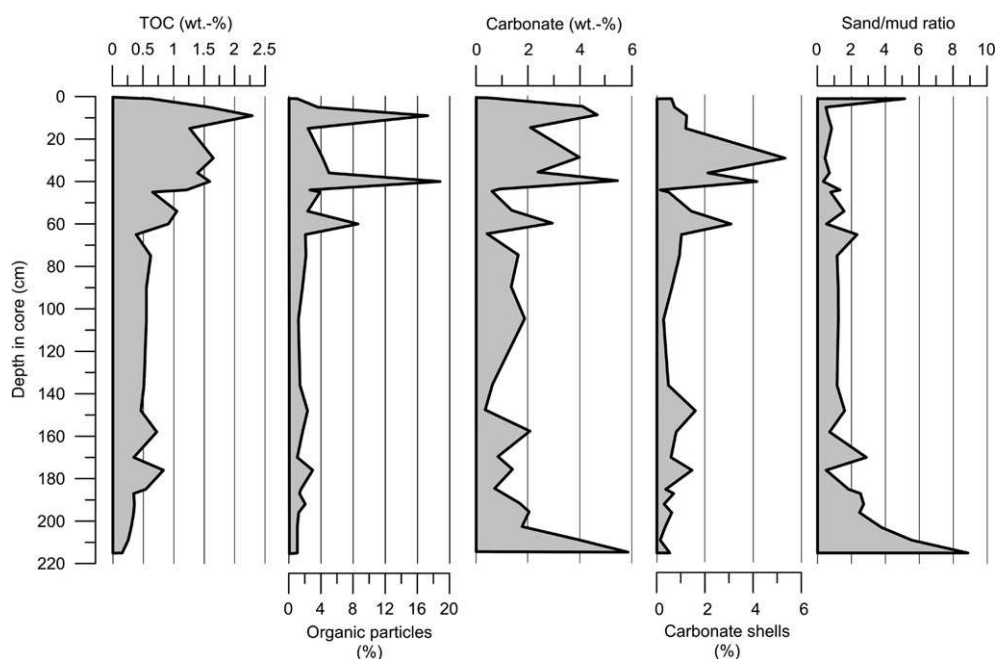


Fig. 5a. Overview of some parameters in core LV-7. The TOC- and carbonate content as well as the abundance of carbonate and organic particles are shown. The variation of grain size in the core is indicated by the sand/mud ratio.

of the counted carbonate shells also show a trend similar to each other but vary greatly in those parts, where the shells exceeded the size of 500 μm and thus were not counted during the component analyses. Maximum carbonate values of 5–6 wt.% are reached at the top and the base of the core. The sand/mud ratio reflects the degree of sediment sorting through the core and indicates transportation and sedimentation processes. Except for the top and the base the ratio varies between one and two illustrating a relatively high mud content in this core. The mud content, however, does not correlate with the abundance of the organic particles or the TOC-content or the carbonate shells whereas peaks in mud content at the top and the base of the core correlate with the carbonate content.

In general the sand fraction (>63 μm) is dominant throughout all four cores. However, some exceptions occur at the top of LV-11, the middle part in Section 1 in LV-2 and the main parts of the upper section in LV-7. The left-hand part in Fig. 5b shows the various distributions of all measured grain sizes throughout the core LV-7. Within the sand fraction the most abundant grain sizes are fine and very fine sand size (250–125 and 125–63 μm). In the upper ~60 cm these two size fractions run parallel to each other. In the lower part, however, the coarser of both size fractions increases and makes up one part of the main grain size fraction next to the fraction 500–250 μm . This development indicates a general fining upward trend within core LV-7.

The following components were identified with varying abundances in the sand fraction (partly shown in Fig. 5b): Quartz (with varying degrees of roundness), gypsum (in three out of four cores), opaque minerals, organic

particles, foraminifers, ostracods, unspecified shell debris, bivalve shells and their debris, gastropods and their debris, debris of echinoderms and crustaceans and fish remnants. Since quartz always represents the predominant component, the abundances of the three quartz-types are shown in the righthand part of Fig. 5b. The degree of roundness (i.e. abrasion) refers to the degree of reworking, to the general source (dust input or river load) or to the duration of the transport (Tucker, 1993): angular quartz is not or little abraded during transport and it is very likely of aeolian origin. Rounded quartz on the other hand is very well abraded either during transport and/or by wave/tide activity. As shown in Fig. 5b, the subrounded quartz type dominates throughout the core. Angular quartz accounts for barely 2% of the counted quartz types and thus shows that the supplied aeolian clastic material gets well abraded due to tide and wave activity in the tidal flat area.

3.2. Facies interpretation

The modern distribution of the sedimentary facies in the study area, as shown in Einsele et al. (1974), is used as a base for the classification of the cores' different facies. Additionally it was taken for the interpretation of the chronological and spatial evolution of the tidal flat sediments. These authors have identified various facies types:

- sandy deposits or mud rich seagrass stands (*Zostera* sp.) below the Mean Low Water-line (MLW),
- accumulations of the large bivalve *Arca senilis* (also known as *Anadara senilis*) or stromatolithic structures directly at the MLW-line,

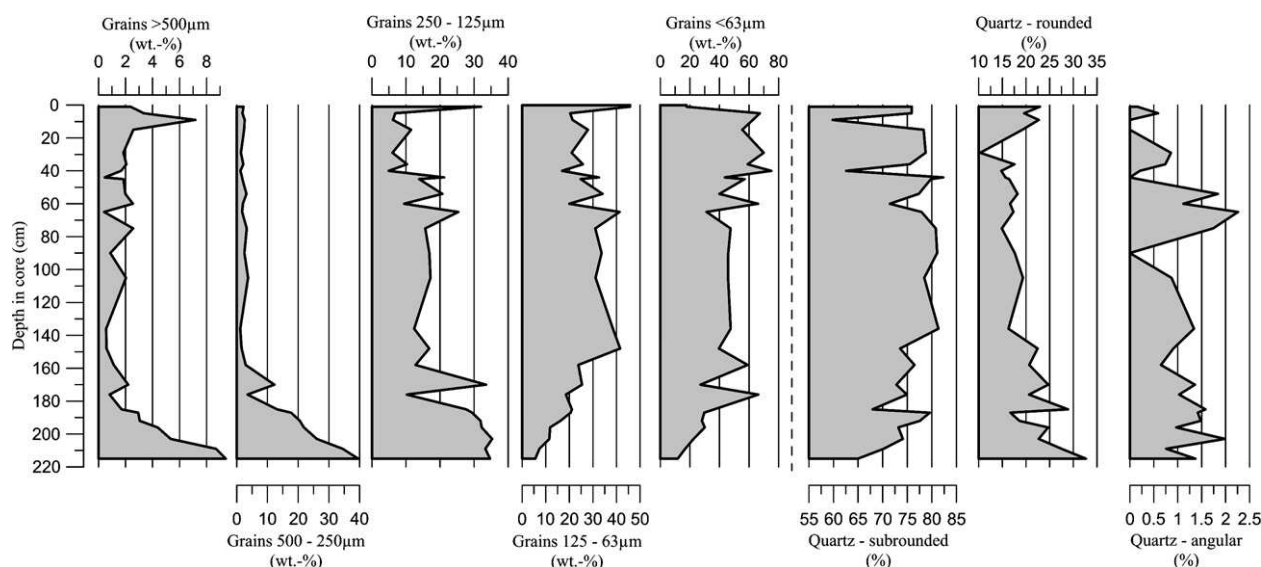


Fig. 5b. Overview of the grain size distribution and quartz grain abundances in core LV-7. The variation of the sediment >63 µm is shown as its subfractions on the left side of the figure. Note the increasing portion of smaller grain sizes towards the top of the core. The three detected quartz morphotypes out of the fraction 500–125 µm and their abundances are shown on the righthand side. The strong dominance of subrounded quartz is noteworthy.

- mud rich seagrass stands (again *Zostera* sp.) or stromatolithic mats between the MLW- and the Mean High Water-line (MHW),
- shell accumulations marking the strand- and MHW-line and finally the adjacent sabkha or sandy deposit with seagrass balls and gastropod shells above the MHW-line.

The occurrence of the various facies types differs: stromatolithic structures are only observed in hypersaline, inner lagoons whereas the seagrass stands and the appearance of *A. senilis* are typical for less saline, protected bays.

According to Koopmann et al. (1979) small carbonate tests such as benthic foraminifers and ostracods cannot be used for detailed facies reconstruction in this area because their appearance is at least partially a function of wave or current activity. Thus they are not considered for the sedimentological interpretation of the cores. A detailed interpretation of the sedimentary inventory of core LV-7 is given here exemplarily (Fig. 6).

- The base of the core is defined as the first facies unit (217 – 205 cm):
 - slightly muddy, medium to fine sand, high carbonate content (~8 wt.%), low TOC-content,
 - echinoderm and crustacean remains as well as worm tubes and all sorts of shells and shell debris,
 - no lamination, the complete unit appears compact/consolidated,
 - light yellowish to light olive brown colour reflecting the low TOC-content,
 - no sharp boundary with the overlying facies indicating a rather smooth transition to the next facies unit.

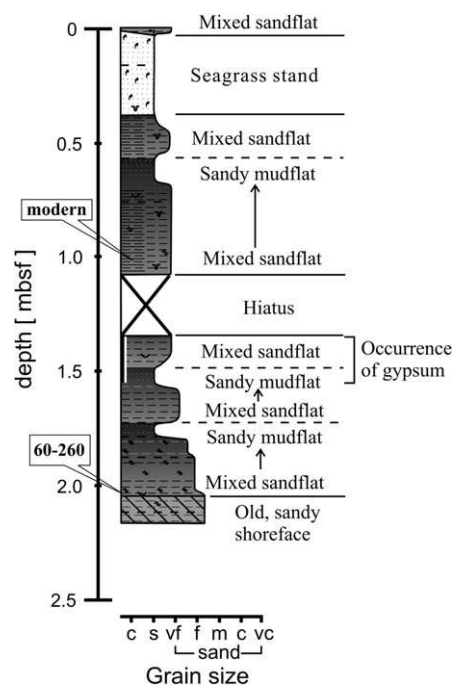


Fig. 6. Schematic overview of the core LV-7. The corresponding age data in 2σ-range is given on the left side. The depth within the core is expressed as meters below sea floor. For key to the symbols and greyscale see Fig. 7.

Based on these observations the lowest part of the core can be interpreted as an *older, sandy shoreface deposit* that evolved in a very shallow water environment. The observed compactness might be due to the exposure as an aerial surface, burial under a sediment load or as a third possibility, transformation by diagenetic processes. The probability of each process will be discussed later in this chapter. The

light colour might indicate either the original lack or the postdepositional decay of organic carbon.

- The second facies unit (205–135 cm):
 - shift towards muddy fine sand being followed by three fining upward trends into sandy mud at ~175, ~155 and ~135 cm,
 - increased carbonate content accompanying the fining upward trends with a decline to a moderate level in the muddy parts, low TOC-content at the base of the unit but increased to a moderate level especially in the muddy parts,
 - intense bioturbation throughout the lower part, slightly visible parallel lamination with alternating sand and mud content in the upper part (<165 cm),
 - occurrence of idiomorphic gypsum crystals with rounded edges in the fraction 1000–500 µm in the upper part (<160 cm).

Stein (1980) found gypsum crystals in surface sediments from the Baie St. Jean and linked them to the adjacent sabkha areas in the hinterland. Shearman (1978) describes mm- to cm-sized, lenticular gypsum crystals growing in algal mats in the intertidal zone as well as large crystals being formed in the adjacent coastal sabkhas of Abu Dhabi at the Trucial Coast (Persian Gulf). In the samples available there is no possibility of distinguishing clearly if those gypsum crystals were either formed in a sabkha on Tidra Island and later flushed into the tidal zone or directly formed in the tidal flat area. At least, their rounded edges indicate short-lasting but secondary transportation.

This unit can be summarised as a *mixed sandflat partially grading into a sandy mudflat* at the top of the fining upward parts. The recurring coarse material at the base of each fining-upward part might be ascribed to the supply of coarser material during strong spring tides. It is also possible that minor storm events flushed this material into the area by redistributing it from other parts of the tidal flat.

- The third facies unit (108–42 cm):
 - very muddy, very fine sand followed by a grading into sandy mud at ~60 cm, two fining upward successions (similar to the ones described for the underlying unit) of which the uppermost one is not completely developed,
 - increase of TOC-content from a medium level to high values in the muddy parts, relatively high carbonate content showing slightly lower values in the muddy portions,
 - fish and crustacean remains might suggest the partial proximity to the MHW-line as being observed in the Baie St. Jean by Stein (1980),
 - clear cross and parallel lamination of dark grey to black and lighter grey layers in the middle and especially upper part indicating a calm environment without burrowing organisms.

In summary this unit can be described as a *mixed sandflat partially grading into a sandy mudflat, similar to the underlying unit but without gypsum crystals*.

- The fourth facies unit (42–4 cm):
 - boundary with the underlying unit cuts off the lamination, appears highly chaotic,
 - rich in TOC (due to accumulations of autochthonous seagrass leaves) and high carbonate content,
 - grain size shifts to predominantly mud and clear bioturbation signatures,
 - fish remains in the middle and lower part may indicate the MHW-line.

Those indications show that this unit represents a *seagrass stand*. Whether it is the one between MLW- and MHW-lines (cf. Einsele et al., 1974) or the one below the MLW-line cannot be proven from the sediment succession. The cause of the development of the seagrass stand in this part of the core remains unclear. Exposure to more light (i.e. just below the MLW-line) of this part of the tidal flat, lessened supply of coarse sediment or reduced tidal current speed might be responsible for the development of the seagrass stand. The grain size shift towards mud in the seagrass stand deposit is typical because the tuft of the seagrass act as a trap for fine sediment in suspension (Bos et al., 2007; Van der Laan and Wolff, 2006).

- The uppermost and fifth facies unit (4–0 cm):
 - very fine to fine sand with remarkably low mud content compared to the underlying sediment facies,
 - drop of TOC-content to a moderate level, low carbonate content,
 - reoccurring fish remains suggesting the proximity to the MHW-line,
 - no visible internal lamination but less chaotic appearance.

Due to these observations and the position of the core in the modern tidal flat area this unit can be summarised as a *mixed sandflat*. A renewed supply of coarser sediments might have buried the seagrass stand.

An age in the range of 60–260 cal yr BP was obtained from material from the mixed sand- to sandy mudflat facies (facies unit two; Fig. 6). This sandflat deposit overlies the basal sandy shoreface deposit and thus the age may mark the approximate beginning of the recent tidal flat deposition in this area. There is an obvious difference in appearance and age of the older, sandy shoreface deposit when compared with the more recent, tidal flat sediments. The compactness of the deposit suggests that these older shoreface sediments could have been subjected to different processes: aerial exposure, burial or diagenetic transformation. The occurrence of the first hypothesis is unlikely since the sea-level did not change significantly during the last 1000 yr and very recent subsidence of the area is not reported

(Barusseau et al., 2007). On the other side, the sea-level curve by Elouard et al. (in Barusseau et al. 1995) shows a decline in sea-level of ca. 1 m ca. 400 yr BP (Fig. 3). Since the shoreface deposit has been found 2–2.5 m below the modern MLW-line and the age data show much older ages for this deposit, this possible sea-level lowstand cannot be connected with the imprinting of this deposit. The deposit still would have been covered by ca. 1.5 m of sea water. Additionally, the most recent research concerning sea-level fluctuations shows a constant course at the modern level for at least the last 3000 yr. Thus aerial exposure seems to have been impossible. The remaining hypotheses of burial or diagenetic overprinting are both likely to have happened, particularly since diagenetic processes are linked with the burial of sediments. But no diagenetic imprints like cementation of grains or etched grain surfaces were observed in the sediment. Thus, mainly burial and possibly an early stage of diagenesis are likely to be the causes for the observed consolidation of this facies unit and its clear differentiation from the overlying, not compacted sediments.

Assuming, that the sandy shoreface deposits that were also found at the bases in two other cores were deposited at roughly the same time, this age shows a gap between the age of the upper sandy shoreface deposit (facies unit one) and the lower, more recent sandflat sediments (facies unit two; see Fig. 7 for all age data). On the one side this gap can be explained by the erosion of sediment during a storm event. The possibility of storm events (marked with stars in Fig. 7) will be discussed in part four. On the other

side, other mechanisms like a temporary very low sedimentation rate or sediment bypassing for this site could be another explanation for this observed pattern. But since the area is exposed within the Golfe and storms occur frequently, it seems likely that these observed deposits are linked to storm events. The second date being within a sand- to mixed sandflat (facies unit three; Fig. 6) indicates that the sediments were deposited approximately in the time span between 1945–1963 A.D. Since this part of the core shows clear lamination the possibility that bioturbation has biased this date can be excluded. So the upper mixed sand- to mudflat as well as the seagrass stand seem to have developed very recently.

Due to the similar appearance of the various facies in the three remaining cores, their interpretations are only briefly summarised here (Fig. 7).

- Core LV-2: Older, sandy shoreface deposit (>80 wt.% of the bulk sediment is of 250–63 μm size, the TOC content is ~0.4 wt.% and the carbonate content is <2 wt.%, unit appears consolidated) – deposit of a possible storm event (marked by an erosive boundary with the underlying unit, an increased supply of material <63 μm that settled after the possible storm surge, mm-sized shells and shell debris being chaotically distributed in this unit and the appearance of carbonate crusts that could have been flushed into the sediment from an adjacent sabkha area) – sandflat – storm deposit (indicated by a high amount (~40 wt.%) of mm-sized, thick walled, partly

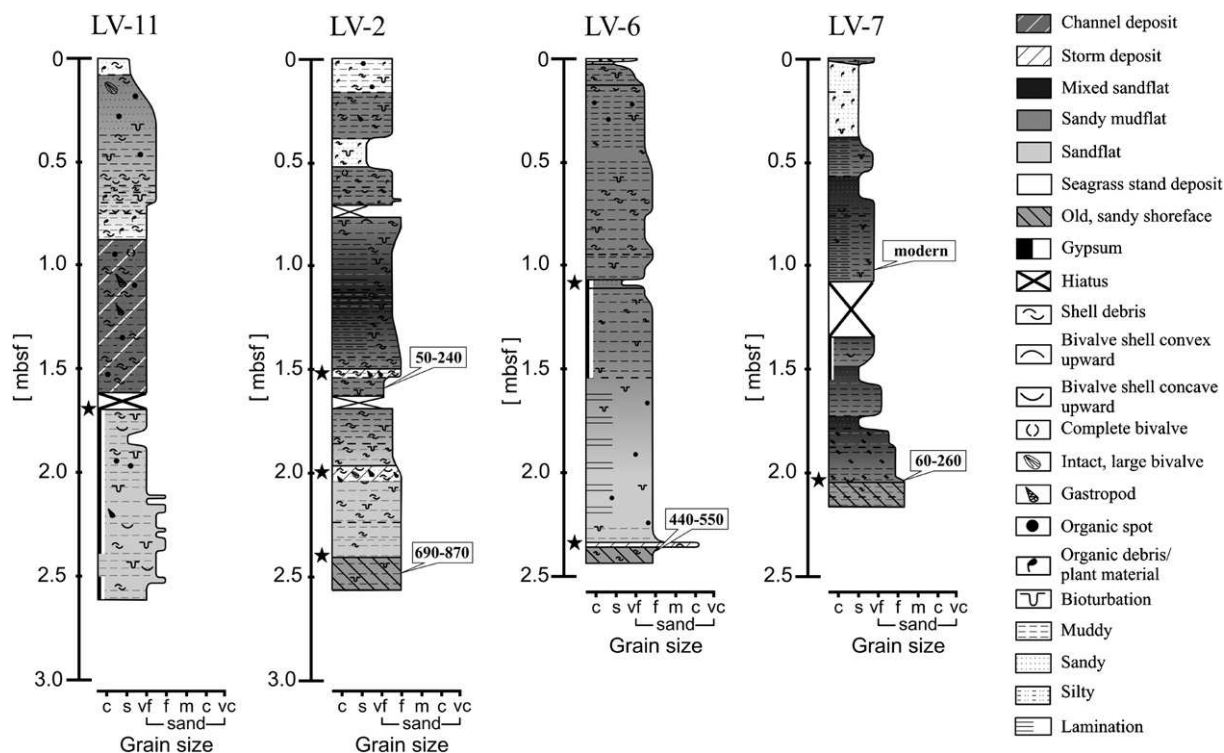


Fig. 7. Overview of the cores. Corresponding ages are given in the 2σ-range at the right side of each core. Symbols within the cores represent different shells, organic fibres or bioturbation. The black stars on the left side of cores mark the clearly detected as well as the assumed storm deposits or sediment gaps due to storm events.

broken, chaotically distributed and freshly preserved gastropod and bivalve shells as well as shell debris in a very pronounced layer and an erosive base that separates this layer from the underlying sediments) – sand- to mixed sandflat – storm layer (increased amount of large shells and shell debris being chaotically distributed, abrupt change of the grain size towards coarser material that might have been flushed in or concentrated during the storm) – mixed sand- to sandy mudflat – mixed sandy flat – seagrass stand – transitional mixed sandflat – seagrass stand.

The *C/N*-ratio (between 6 and 10) shows a marine organic material signal throughout the whole core. An age date at 248 cm in the range of 690–870 cal yr BP from the basal sandy shoreface deposit (Fig. 7) also marks the chronological discrepancy and thus the stratigraphic hiatus between the sedimentation of the older shoreface and the more recent tidal flat deposits. A second age, from 159 cm originating from a mixed sandflat facies directly beneath a storm layer (Fig. 7), dates in the range of 50–240 cal yr BP. It is conceivable that the storm, which produced this layer, eroded parts of the underlying mixed sandflat deposits. Thus this storm deposit is surely slightly younger than this radiocarbon age suggests. On the other hand this age marks the oldest probable date when this storm event could have occurred.

- Core LV-6: Older, sandy shoreface deposit (fraction <63 μm accounts for ~ 3 wt.% within the bulk sediment, the TOC content is <0,2 wt.% and the carbonate content is <1 wt.%, the unit appears consolidated) – storm layer (showing an erosive base to the underlying unit as well as large shells and shell debris and an increased input of material <63 μm similar to the lowest storm deposit in core LV-2) – sandflat grading into mixed sandflat – a possible storm deposit (erosive base, large shells and shell debris and increased input of material <63 μm) – mixed sandflat.

This core provides an age of 440–550 cal yr BP at 239 cm, at the top of the sandy shoreface deposit (Fig. 7). This age, compared with the other dates and their position in the cores, shows again that there is a temporal gap between the sedimentation of the sandy shoreface and the more recent tidal flat deposits.

- Core LV-11: sandflat with a possible close-by sabkha (many gypsum crystals of varying size, remarkable, mm-sized crystals) – channel deposit (mainly gastropod shells being aligned with the horizontal plane in the core indicating a definite water flow) – seagrass stand – mixed sandflat with *A. senilis* ground (indicating the deposition of this facies unit close to the MLW-line) – seagrass stand.

No ages are available for this core but the sedimentary succession does show a similar facies at its base (sandflat

with gypsum) as observed in cores LV-6 and LV-7. Assuming this similarity the tidal flat development in the area represented by the core may have commenced around 60–260 cal yr BP.

4. Sedimentary history of the area around Tidra Island

The development of the area within the past ~ 800 years shows, that the tidal flat environment has undergone clear changes within a few centuries. Those dynamic conditions affect this system's value as an ecosystem. When compared with the northern part of the Golfe's coast it is remarkable that Tidra Island and the surrounding tidal flat area morphologically protrude. In this way, they are exposed to the mainly northerly water currents in the Golfe d'Arguin (Fig. 1) and different sedimentation process can be expected when compared with the remaining coast. Sediment bypassing or accumulation is reflected by the smoothed course of large parts of the coast in the Golfe but in a tidal flat system, erosion, redistribution and accumulation are equally important. The tidal flat area around the Tidra Island seems to have evolved into its fully developed stage in the last ~ 800 yr which indicates, that the character of this part of the coast has changed. This could be due to various reasons. One cause could be the further expansion of the tidal inlet east of Tidra Island which plays a major role in local sediment distribution. First it interrupts the direct sediment supply of sand from the coastal dunes onto Tidra Island and the western part of the tidal flat area and second it shapes the east coast of Tidra Island by tidal and wave activity. Other causes can be the creation and movement of local sand bars which block or produce channel systems that drain then alternating areas. A further cause could be the long-term change in strength or course of the hydrological currents on the Golfe d'Arguin. Peters (1976) states, that the in- and outflow along the edge of the Golfe can change and observations have shown, that the circulation of the water masses on the Golfe can show completely different patterns than observed by this author. It thus seems likely, that changes in the circulation pattern affect the sedimentation and thus the shape of the coast and its surrounding area.

A shallow water area like the tidal flats around Tidra Island is especially sensitive to conditions that occur during storm events such as deeper wave bases that are able to rework the upper sediments and thus reshape the area. Storm deposits with varying thicknesses and different internal structures are observed in tidal flats around the world (e.g. Sha, 1990; Weidong et al., 1997). Their recognition within the sediment record is difficult when the textural inventory has been secondarily destroyed by bioturbation or the typical, internal structures are not clearly visible. Furthermore, the characteristics of storm deposits can vary widely depending on the local bathymetry and sedimentary characteristics as well as meteorological conditions. Additional to the fact that storms can cause typical deposits, single storm events have the potential to erode large parts

of the coastal area. This, for example, has been observed in the German Wadden Sea with the sediment being transported out of the tidal flat area and deposited in the open sea (Streif, 1990). Especially remarkable is the storm event in A.D. 1362 during which ca. 74 km² of the coastal area in the Harle region were lost to the sea (Ladage and Stephan, 2004).

Storms with a wind direction of North to Northeast/East occur frequently especially in the first half of the year along the NW-African margin (e.g. Middleton, 1987; Dedah, 1993; Bozzano et al., 2002) so it is likely that they influence the shallow water sedimentation in the Banc d'Arguin. We therefore expect that the storm layers found in the proximity of Tidra Island might be an evidence of at least local reorganisation of the tidal flat sediments. Within two out of the four cores, an assumed series of numerous possible storm events seems to have left two slightly different deposits. The sediment succession in core LV-2 shows two storm deposits of one type having the following characteristics: an erosional base to the underlying unit and a high input of large (>1000 µm) shells and shell debris that are chaotically arranged. There are no typical structures visible but this can be due to postdepositional bioturbation which has frequently been observed. The second type of storm deposit especially preserved in core LV-6 (at ~110 cm) has a similar appearance but with a lesser amount of large shells and shell debris as well as an increased content of mud. This mud is possibly the result of the surge being associated with the storm. The flooding probably redistributed fine sediment into the area of core LV-6 in which normally coarser grained sediments accumulate.

In cores LV-7 and LV-11 there are no storm deposits detected but this observation does not necessarily prove the absence of storm-related imprints in these cores. The transition from consolidated, medium sand (unit one) towards loose, fine sand (unit two) in core LV-7 correlates with the pronounced storm deposit in LV-6. Thus it is suggested that the described transition is rather a stratigraphical and thus chronological gap due to sediment erosion. After the storm, the normal tidal flat sedimentation could have been re-established and filled the space being left by the eroded sediment. As a result the sedimentary pile appears transitional. Since core LV-11 does not show the pronounced sandy shoreface at the base, the correlation of the core with the three remaining ones is speculative. It appears though that the development of the channel on top of the sandflat deposit was possible because of an erosional storm event in this part of the area that shows a similar pattern (no deposit, purely erosive) to the one being observed at the base of core LV-7. The assumption is that during the storm the sediment was incised and thus provided a pathway for the tidal currents which gradually produced the observed channel deposit.

The obvious difference in the storm deposits in cores LV-11 & LV-7 from the ones in cores LV-2 & LV-6 could be explained by their position within the tidal flat area

around Tidra Island. The last two cores were taken in areas (Fig. 2) that are directly exposed to the storm waves coming from the North to Northeast. Thus, those core locations might be more affected by sediment resuspension and post-storm deposition than the more sheltered areas.

Considering those observed storm events within the worldwide climatic context of the late Holocene it is worth mentioning that the cores' succession covers the time span of the LIA that ranged from ~650–80 cal yr BP. It is thus possible that the cooler climatic conditions, observed mainly in the northern hemisphere (e.g. Gasse, 2000; Gasse, 2005; Hunt, 2006), could have also affected the investigated region. As described in chapter 1.2, there are observations of lower sea surface temperatures as well as reduced seasonality in the area off Cap Blanc. These phenomena are ascribed to an increased supply of colder water masses from the north as well as an enhanced upwelling along the coast of W.-Africa (DeMenocal et al., 2000). These observations in turn are linked to the intensification of the northerly trade winds in this time period which possibly also shifted the Intertropical Convergence Zone (ITCZ) southwards (Nguetsop et al., 2004). These likely, intensified trade winds and related storm events could have produced the storm deposits that were mainly found in the middle parts of the cores. But this idea remains highly speculative and would require further field studies.

5. Conclusion

The combined sedimentological and geochemical analyses of the sediment cores located in the proximity of Tidra Island, Banc d'Arguin, allowed the identification of four main sedimentary facies types in the cores' non-continuous successions: an older, sandy shoreface deposit; more recent sand- to mudflat deposits with various intercalated stages, as well as seagrass stands and storm deposits.

Three cores show sandy shoreface deposits at their base suggesting that the large, very shallow area in the proximity of Tidra Island had already developed at ca. 800 cal yr BP. Later, catastrophic as well as partly continuous erosion, local relocation and deposition of sediments have reshaped the area and formed the modern tidal flat deposits that are observed in all cores. Especially the erosion of sediments during storms produced new accommodation space in the water column. The begin of the tidal flat development on top of the sandy shoreface deposits in the lowermost parts of the cores is marked with such an erosive storm event. The character of the tidal flats varies locally from sandflat in the proximal area of Tidra Island to mixed sand- to sandy mudflat in the distal, western area off the Tidra Island. Seagrass stands are observed only in the youngest deposits, which might be due to formerly inhospitable conditions.

Acknowledgement

We thank Rüdiger Stein for giving many useful comments. We are grateful to the team who took the cores in

Mauritania (P. Costa, S. Vilanova and J. Dinis) and to the staff of the PNBA at the Iwik Station. The coring campaign was partially funded by ICSU-Dark Nature and IGCP490. Furthermore we would like to thank the staff of the Department Geography and Earth Sciences, Brunel University for their help in London. We acknowledge Thomas Vestring and the Radiological Department of the Diakonikerkrankenhause Rotenburg for technical support. In addition, we thank the two anonymous reviewers for their helpful comments and Mike Turner from Brunel University for the proof-reading. This is RCOM contribution no. 0537.

References

- Bard, E., 1988. Correction of accelerator mass spectrometry ^{14}C ages measured in planktonic foraminifera: paleoceanographic implications. *Paleoceanography* 3 (6), 635–645.
- Barusseau, J.P., Bâ, M., Descamps, C., Diop, E.H.S., Giresse, P., Saos, J.-L., 1995. Coastal evolution in Senegal and Mauritania at 10^3 , 10^2 and 10^1 -year scales: natural and human records. *Quaternary International* 29/30, 61–73.
- Barusseau, J.P., Vernet, R., Saliège, J.F., Descamps, C., 2007. Late Holocene sedimentary forcing and human settlements in the Jerf el Oustani – Ras el Sass region (Banc d'Arguin, Mauritania). *Geomorphologie-Relief Processus Environnement* 1, 7–18.
- Bos, A.R., Bouma, T.J., de Kort, G.L.J., van Katwijk, M.M., 2007. Ecosystem engineering by annual intertidal seagrass beds: Sediment accretion and modification. *Estuarine, Coastal and Shelf Science* 74, 334–348.
- Bozzano, G., Kuhlmann, H., Alonso, B., 2002. Storminess control over African dust input to the Moroccan Atlantic margin (NW Africa) at the time of maxima boreal summer insolation: a record of the last 220 kyr. *Palaeogeography, Palaeoclimatology, Palaeoecology* 183, 155–168.
- Dahdouh-Guebas, F., Koedam, N., 2001. Are the northernmost mangroves of West Africa viable? – a case study in Banc d'Arguin National Park, Mauritania. *Hydrobiologia* 458, 241–253.
- Dedah, S.Ould, 1993. Wind, surface water temperature, surface salinity and pollution in the area of the Banc d'Arguin, Mauritania. *Hydrobiologia* 258 (1–3), 9–19.
- Dekker, R., Beukema, J.J., 1999. Relations of summer and winter temperatures with dynamics and growth of two bivalves, *Tellina tenuis* and *Abra tenuis*, on the northern edge of their intertidal distribution. *Journal of Sea Research* 42 (3), 207–220.
- DeMenocal, P., Ortiz, J., Guilderson, T., Sarnthein, M., 2000. Coherent high- and low-latitude variability during the Holocene Warm Period. *Science* 288, 2189–2202.
- Domain, F., 1977. Carte sédimentologique du plateau continental sénégalais. Extension à une partie du plateau continental de la Mauritanie et de la Guinée Bissau. O.R.S.T.O.M., Paris.
- Einsle, G., Herm, D., Schwarz, H.U., 1974. Holocene eustatic (?) sea level fluctuation at the coast of Mauritania. “Meteor” Forschungsergebnisse, Reihe C (18), 43–62.
- Elouard, P., Faure, H., Hebrard, L., 1969. Quaternaire du littoral mauritanien entre Nouakchott et Port-Etienne (18°21' latitude Nord). In: Gowthorpe, P. (Ed.), 1993. Une visite au Parc national du Banc d'Arguin. Publication of Parc National du Banc d'Arguin, Nouakchott, Mauritanie, pp. 48–74.
- Fretter, V., Graham, A., 1981. *Calyptrea chinensis* (Linnaeus, 1758), Chinaman's hat. *Journal of Molluscan Studies* 47, 314–317, and 286–289.
- Gasse, F., 2000. Hydrological changes in the African tropics since the last glacial maximum. *Quaternary Science Reviews* 19, 189–211.
- Gasse, F., 2005. Continental paleohydrology and paleoclimate during the Holocene. *Comptes Rendus Geoscience* 337, 79–86.
- Hunt, B.G., 2006. The medieval warm period, the little ice age and simulated climatic variability. *Climate Dynamics* 27 (7–8), 677–694.
- Koopmann, B.J., Lees, A., Piessens, P., Sarnthein, M., 1979. Skeletal carbonate sands and wind-derived silty marls off the Saharan coast: Baie du Lévrier, Arguin Platform, Mauritania. “Meteor” Forschungsergebnisse, Reihe C (30), 15–57.
- Ladage, F., Stephan, H.J., 2004. Morphologische Entwicklung im Seegat Harle und seinem Einzugsgebiet. Report by order of the Niedersächsisches Landesamt fuer Oekologie, Forschungsstelle Kueste, Norderny. (in German).
- Levin, I., Kromer, B., Schoch-Fischer, H., Bruns, M., Berdau, D., Vogel, J.D., Munnich, K.O., 1985. 25 years of tropospheric ^{14}C observations in Central Europe. *Radiocarbon* 27 (1), 1–19.
- Manning, M.R., Lowe, D.C., Melhuish, W.H., Sparks, R.J., Wallace, G., Brenninkmeijer, C.A.M., McGill, R.C., 1990. The use of radiocarbon measurements in atmospheric studies. *Radiocarbon* 32 (1), 37–58.
- Michaelis, H., Wolff, W.J., 2001. Soft-bottom fauna of a tropical (Banc d'Arguin, Mauritania) and a temperate (Juist Area, German North Sea Coast) intertidal area. In: Reise, K. (Ed.), *Ecological comparisons of sedimentary shores*, Ecological Studies (151). Springer, Berlin, pp. 55–274.
- Middleton, N.J., 1987. Desertification and wind erosion in the western Sahel: The example of Mauritania. Research paper no. 40, School of Geography, University of Oxford, pp. 1–26.
- Nguetsop, V.F., Servant-Vildary, S., Servant, M., 2004. Late Holocene climatic changes in west Africa, a high resolution diatom record from equatorial Cameroon. *Quaternary Science Reviews* 23, 591–609.
- Peters, H., 1976. The spreading of the water masses of the Banc d'Arguin in the upwelling area off the northern Mauritanian coast. “Meteor” Forschungsergebnisse, Reihe A (18), 78–100.
- Piessens, P., 1979. Influence relative des sources de production et du transport dans la formation de faciès calcaires biogéniques: les sédiments quaternaires de la Plate – forme d'Arguin (Mauritanie) et comparaison avec des régions côtières européennes (Irlande et Hébrides). Ph.d. thesis, Univ. Louvain (in French).
- Puig, P., Ogston, A.S., Guillén, J., Fain, A.M.V., Palanques, A., 2007. Sediment transport processes from the topset to the foreset of a crenulated clinoform (Adriatic Sea). *Continental Shelf Research* 27, 452–474.
- Roberts, N., 1989. *The Holocene – An environmental history*. Blackwell Publishing, first ed. Oxford & Cambridge. 227 pp.
- Sevrin-Reyssac, J., 1993. Hydrology and underwater climate of the Banc d'Arguin, Mauritania: a review. *Hydrobiologia* 258 (1–3), 1–8.
- Sha, L.P., 1990. Surface sediments and sequence models in the ebb-tidal delta of Texel Inlet, Wadden Sea, The Netherlands. *Sedimentary Geology* 68, 125–141.
- Shearman, D.J., 1978. Evaporites of coastal sabkhas. In: Dean, W.E., Schreiber, B.C. (Eds.), *Marine evaporates. Lecture notes for short courses* (4). Society of Economic Paleontologists and Mineralogists, Oklahoma City.
- Stein, R., 1980. Sedimentverhältnisse in der Baie St. Jean. Diplom thesis. Univ. Kiel. (in German).
- Streif, H., 1990. Das ostfriesische Küstengebiet. Sammlung geologischer Fuehrer 57, Gebr. Borntraeger, second edition, Berlin, Stuttgart. (in German).
- Stuiver, M. and Reimer, P.J., 1998. CALIB Version 4.0 [Computer program] URL <http://depts.washington.edu/qil/>.
- Tucker, M., 1993. *Sedimentary rocks in the field*. John Wiley & Sons, Chichester, 153pp.
- Van der Laan, B.B.P.A., Wolff, W.J., 2006. Circular pools in the seagrass beds of the Banc d'Arguin, Mauritania, and their possible origin. *Aquatic Botany* 84, 93–100.

- Weidong, D., Baoguo, Y., Xiaogen, W., 1997. Studies of strom deposits in China: a review. *Continental Shelf Research* 17 (13), 1645–1658.
- Wolff, W.J., Smit, C.J., 1990. The Banc d'Arguin, Mauritania, as an environment for coastal birds. *Ardea* 78, 17–38.
- Wolff, W.J., Duiven, A.G., Duiven, P., Esselink, P., Gueye, A., Meijboom, A., Moerland, G., Zegers, J., 1993a. Biomass of macrobenthic tidal flat fauna of the Banc d'Arguin, Mauritania. *Hydrobiologia* 258 (1–3), 151–163.
- Wolff, W.J., van der Land, J., Nienhuis, P.H., de Wilde, P.A.W.J., 1993b. The functioning of the ecosystem of the Banc d'Arguin, Mauritania: a review. *Hydrobiologia* 258 (1–3), 211–222.